

Correlation and trust mechanism-based rumor propagation model in complex social networks

Xian-Li Sun(孙先莉), You-Guo Wang(王友国), and Lin-Qing Cang(仓林青)
Citation: Chin. Phys. B, 2022, 31 (**5**): 050202. DOI: 10.1088/1674-1056/ac3d82
Journal homepage: http://cpb.iphy.ac.cn; http://iopscience.iop.org/cpb

What follows is a list of articles you may be interested in

Dynamics and intermittent stochastic stabilization of a rumor spreading model with guidance mechanism in heterogeneous network

Xiaojing Zhong(钟晓静), Yukun Yang(杨宇琨), Runqing Miao(苗润青), Yuqing Peng(彭雨晴), and Guiyun Liu(刘贵云)
Chin. Phys. B, 2022, 31 (**4**): 040205. DOI: 10.1088/1674-1056/ac587d

Ultra-broadband absorber based on cascaded nanodisk arrays

Qi Wang(王琦), Rui Li(李瑞), Xu-Feng Gao(高旭峰), Shi-Jie Zhang(张世杰), Rui-Jin Hong(洪瑞金), Bang-Lian Xu(徐邦联), and Da-Wei Zhang(张大伟)
Chin. Phys. B, 2022, 31 (**4**): 040203. DOI: 10.1088/1674-1056/ac2d1d

Anti-function solution of uniaxial anisotropic Stoner-Wohlfarth model

Kun Zheng(郑坤), Yu Miao(缪宇), Tong Li(李通), Shuang-Long Yang(杨双龙), Li Xi(席力), Yang Yang(杨洋), Dun Zhao(赵敦), and De-Sheng Xue(薛德胜)
Chin. Phys. B, 2022, 31 (**4**): 040202. DOI: 10.1088/1674-1056/ac401e

Dynamics and near-optimal control in a stochastic rumor propagation model incorporating media coverage and Lévy noise

Liang'an Huo(霍良安) and Yafang Dong(董雅芳)
Chin. Phys. B, 2022, 31 (**3**): 030202. DOI: 10.1088/1674-1056/ac2f35

Dynamics of a stochastic rumor propagation model incorporating media coverage and driven by Lévy noise

Liang-An Huo(霍良安), Ya-Fang Dong(董雅芳), and Ting-Ting Lin(林婷婷)
Chin. Phys. B, 2021, 30 (**8**): 080201. DOI: 10.1088/1674-1056/ac0423

Correlation and trust mechanism-based rumor propagation model in complex social networks

Xian-Li Sun(孙先莉), You-Guo Wang(王友国)†, and Lin-Qing Cang(仓林青)

School of Science, Nanjing University of Posts and Telecommunications, Nanjing 210023, *China*

(Received 5 August 2021; revised manuscript received 2 November 2021; accepted manuscript online 26 November 2021)

In real life, the rumor propagation is influenced by many factors. The complexity and uncertainty of human psychology make the diffusion model more challenging to depict. In order to establish a comprehensive propagation model, in this paper, we take some psychological factors into consideration to mirror rumor propagation. Firstly, we use the Ridenour model to combine the trust mechanism with the correlation mechanism and propose a modified rumor propagation model. Secondly, the mean-field equations which describe the dynamics of the modified SIR model on homogenous and heterogeneous networks are derived. Thirdly, a steady-state analysis is conducted for the spreading threshold and the final rumor size. Fourthly, we investigate rumor immunization strategies and obtain immunization thresholds. Next, simulations on different networks are carried out to verify the theoretical results and the effectiveness of the immunization strategies. The results indicate that the utilization of trust and correlation mechanisms leads to a larger final rumor size and a smaller terminal time. Moreover, different immunization strategies have disparate effectiveness in rumor propagation.

Keywords: rumor propagation model, Ridenour model, immunization strategy

PACS: 02.60.Cb, 89.75.–k, 87.23.Ge **DOI:** 10.1088/1674-1056/ac3d82

1. Introduction

In the era of the information explosion, the online social network has become an indispensable platform for people to exchange information, share files, and communicate.[1] When people use online social media to enjoy convenient and efficient information services, some rumors may spread rapidly on the Internet. Rumor refers to some statements whose truth-value are unverifiable or deliberately false. Hence, the spread of rumors may induce substantial economic loss or widespread social panic within a short time.[2] For instance, a loss of 130 billions in stock value occurred after a false twitter declared that Obama was injured in an explosion.[3] Consequently, it is necessary to analyze the rumor spreading process. Meanwhile, appropriate measures should also be adopted to impede the rumor diffusion to minimize the damages and losses to people and society.[4]

Up to now, researchers in mounting numbers have conducted extensive researches on rumor propagation. The bulk of rumor diffusion models have been investigated on the basis of epidemic spreading models because of many similar features between the two forms of transmission.[5,6] A portion of scholars tried their best to extend the standard SIR model[7] to other complicated models, including the SEIR diffusion model,[8] DI-SCIR model,[9] SHIR mode,[10] ISCR rumor spreading model,[11] etc. Li *et al.*[12] considered that the node of the Hibernator coming from the spreaders due to forgetting factors and later becoming spreaders again was introduced in the diffusion model. Huang *et al.*[13] came up with the SIRaRu model, which classifies stiflers into two groups based on their attitudes to rumors. Xia *et al.*[14] introduced a new authoritative state who spread the authoritative information into the SIAR model. Currently, some scholars have turned to study the impact of human psychological factors and social phenomena in rumor spreading, so they came up with many new mechanisms, such as refutation mechanism,[15] perception mechanism,[16] social reinforcement mechanism,[17] etc. Zhao *et al.*[18] found that the forgetting rate can affect rumor spreading, so they added the forgetting mechanism into the SIR model. Afassinou[19] came up with the education mechanism to differ the spreading probability of nodes with different educational extent. Besides, scholars also considered different influencing factors, such as birth rate and death rate,[20] group propagation,[21] the activity of spreaders,[22] etc. Moreover, the degree of trust is an important influence for people to spread rumors. Zhang *et al.*[23] combined the information diffusion with the trust relationship among people and calculated the probability that individuals believe rumors based on the trust degree. Chen *et al.*[24] came up with a rumor diffusion model, based on a two-level-mixing SIR model and the modified trust degree. Jin *et al.*[25] considered the information receiver's subjective initiative and constructed a rumor diffusion model based on content trust. Zhu *et al.*[26] constructed the rumor spreading model, considering the trust mechanism, and combined it with the SEIR model. Chua *et al.*[27] analyzed the extent of users' trust when facing rumors and studied two kinds of rumors. Liu *et al.*[28] regarded that two influential factors in the process of rumor spreading are the trust degree of the source node and rumor explosion de-

†Corresponding author. E-mail: wangyg@njupt.edu.cn

© 2022 Chinese Physical Society and IOP Publishing Ltd

gree. A modified SIR model, including the trust mechanism, was established to make the process of diffusion fit the realistic cases more closely by Wang *et al.*[29] Furthermore, rumor diffusion also depends on the relationship of individuals and the characteristic of rumors' features. Singh *et al.*[30] studied the impact of degree–degree correlation in rumor diffusion. Chen *et al.*[31] introduced the correlation coefficient into the rumor spreading model, which describes the extent of correlation between people's daily life and the rumor.

In addition, the study of immunization strategy is an essential part of rumor spreading, which can control the level of rumor diffusion. Random immunization,[32] targeted immunization,[33] acquaintance immunization[34] and active immunization[35] are the common control strategies. Nian *et al.*[36] considered random immunization based on node activity, in which the node with most active is immunized firstly. Wang *et al.*[37] discussed the random immunization and targeted immunization strategies in detail and obtained the related thresholds in homogeneous and heterogeneous networks. Cohen *et al.*[38] put forward the acquaintance immunization firstly which requires no knowledge of global information and topology. Zhu *et al.*[39] investigated active immunization and deduced the immunization threshold.

In previous research works, they usually considered one mechanism in the diffusion process. Nevertheless, the characteristics of users' behaviors are very complicated. In the real world, spreaders do not always choose trusted individuals to spread rumors but tend to deliver messages to someone related to rumors even though there is no strong bond between two individuals. For example, if someone gets a rumor related to his favorite celebrity, he will be more inclined to spread the rumor firstly to individuals who also love the celebrity.[40] Hence, the degree of intimacy between nodes is not the only factor to be considered during the spreading process. Besides, the degree of relevance between the neighbor nodes and the rumor is an essential factor to be considered in rumor diffusion. In an attempt to generalize the rumor spreading process realistic, in this paper, we come up with a correlation mechanism and use the Ridenour model[41] to combine the trusted mechanism with the correlation mechanism. We establish the mean-field equations to depict the modified SIR model on homogenous and heterogeneous networks based on two mechanisms. Then, we conduct a steady-state analysis for spreading thresholds and the final rumor sizes. Next, we investigate immunization strategies and obtain immunization thresholds. Moreover, simulations on different networks are carried out to validate the above theoretical results and the effectiveness of immunization strategies. Finally, we perform a parallel comparison of different immunization strategies in BA scale-free network.

The rest of this paper is organized as follows. In Section 2, we combine two mechanisms by the Ridenour model. In Section 3, we analytically research the modified SIR model on homogenous and heterogeneous networks in detail. Next, effective immunization strategies are investigated to deduce immunization thresholds in Section 4. In Section 5, simulations are carried out to verify the conclusions obtained in previous sections. Lastly, conclusions are presented in Section 6.

2. The combination of two mechanisms by the Ridenour model

A social network composed of a variety of $N = |V|$ nodes and a series of E edges that connect pairs of nodes can be represented as a directed graph $G = \{V, E\}$. At per time step, individuals in networks can be separated into three states: ignorant (I), spreader (S), and stifler (R). To be more specific, the above three kinds of individuals stand for someone who has never received the rumor, who is spreading the rumor, and who has heard the rumor but refused to diffuse it, respectively. Figure 1 describes the process of the modified SIR model for three states changing.

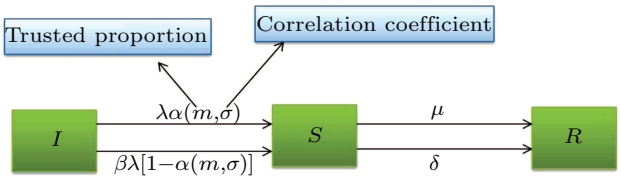


Fig. 1. Structure of the modified SIR rumor spreading process. σ is the correlation coefficient, m is the trusted proportion, α is the sum proportion of trusted and related neighbors.

We divide the diffusion direction into two categories. One is spreaders transmit rumors to trusted or related neighbors and the other is to untrusted or unrelated neighbors. If a neighbor is not only a trusted but also a related person, for convenience, we classify the neighbor to a trusted neighbor to avoid double counting. According to the research of Robin Dunbar,[42] the restricted neocortical neurons limit the human's information-processing capacity, leading to an individual cannot monitor tangled interpersonal relationships simultaneously. To be more specific, an individual will have a stable social network of 150 people, and the number of in-depth contacts is about 20 people.[43] This is the famous "Dunbar number". Therefore, we calculate the value of the trusted proportion $m = 2/15 \approx 0.13$. Thus, we can suppose that each node has the same proportion of trusted neighbor nodes. Moreover, σ $(0 < \sigma < 1)$ is the correlation coefficient that can judge the extent to which a rumor is related to our life. The bigger correlation coefficient is, the more related neighbor nodes are. Then, we use $\alpha(m, \sigma)$ to represent the sum proportion of trusted and related neighbors, and the proportion of untrusted and unrelated is $1 - \alpha(m, \sigma)$.

Next, we will discuss how to combine the trust mechanism with the correlation mechanism. The Ridenour model is

one of the common growth curves and is often used to predict the development of new technologies and the sales of new products.[41,44] The general form of its mathematical model is shown below:

$$N(t) = \frac{L}{1+(\frac{L}{N_0}-1)\,\mathrm{e}^{-bt}}, \quad (t \geq t_0, b > 0),$$

where $N(t)$ is the number of people who are familiar with new productions or technologies. When $t = t_0$, N_0 represents the initial people who know new products or technologies. Moreover, b is a correction factor and L means the limit of $N(t)$. In social networks, suppose a node with k degree, along with the increase of σ, $L = \lim_{\sigma\to 1} N(\sigma) = k$. When $\sigma = 0$, the system only considers trust mechanism, so we can obtain $N_0 = mk$. Consequently, the sum proportion of the trust and related people is described by

$$\alpha(m,\sigma) = \frac{k}{[1+(\frac{k}{mk}-1)\,\mathrm{e}^{-b\sigma}]k} = \frac{1}{1+(\frac{1}{m}-1)\,\mathrm{e}^{-b\sigma}} = \alpha, \quad (\sigma \geq 0, \quad b > 0). \tag{1}$$

Figure 2 presents the change of the sum proportion of the trust and related people. Clearly, given a fixed σ, α increases as m increases. When m is a fixed value, the sum proportion α is proportionate to the increased correlation coefficient σ. Visually, the tendency of the sum proportion α is approximately identical to different values of the correction factor.

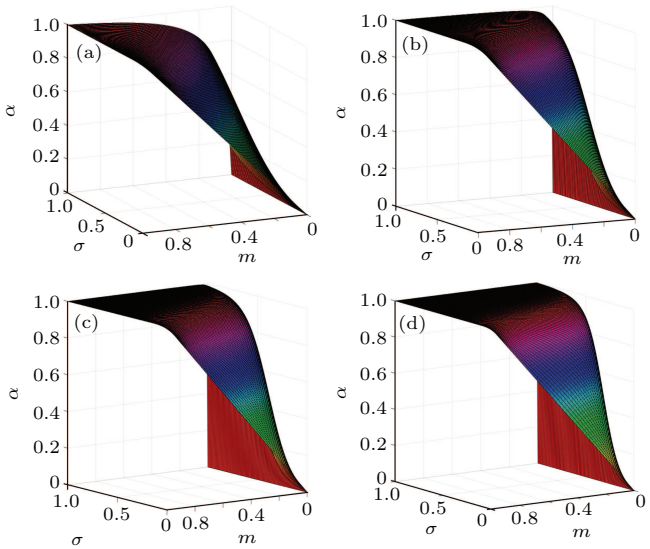


Fig. 2. Structure of the Ridenour curve. The sum proportion of the trust and related people is shown as a function of m and σ for different values of b: (a) $b = 3$, (b) $b = 6$, (c) $b = 9$, (d) $b = 12$.

3. A modified SIR rumor propagation model

In complex social networks, the transmission course is shown in Fig. 1 and the corresponding rules of the modified SIR rumor can be generalized as below:

(1) An ignorant contact with a trusted or related spreader at a rate $\alpha(m,\sigma)$, the ignorant might change to a spreader with probability λ. By contrast, if an ignorant contacts an unrelated and untrusted spreader at a rate $1-\alpha(m,\sigma)$, the ignorant will be infected with probability $\beta\lambda$.

(2) A spreader in contact with a stifler or another spreader during the process of rumor propagation will become a stifler at a rate μ.

(3) A spreader spontaneously forgets the rumor because of time and other influencing factors at a rate δ.

3.1. Homogeneous modified SIR model

To realize more characteristics of the modified rumor model, we firstly focus on homogeneous networks whose degree fluctuations are tiny and there are no correlations among nodes. The three states satisfy the following condition:

$$I(t) + S(t) + R(t) = 1.$$

Based on two mechanisms, the new mean-field equations for changing density of different nodes can be established as shown below:

$$\frac{\mathrm{d}I(t)}{\mathrm{d}t} = (-\lambda\alpha - \beta\lambda + \beta\lambda\alpha)\langle k\rangle I(t)S(t), \tag{2}$$

$$\frac{\mathrm{d}S(t)}{\mathrm{d}t} = (\lambda\alpha + \beta\lambda - \beta\lambda\alpha)\langle k\rangle I(t)S(t) - \mu\langle k\rangle S(t)[S(t)+R(t)] - \delta S(t), \tag{3}$$

$$\frac{\mathrm{d}R(t)}{\mathrm{d}t} = \mu\langle k\rangle S(t)[S(t)+R(t)] + \delta S(t), \tag{4}$$

where $\langle k\rangle$ represents the average degree of homogeneous network. In the beginning, we assume that the system only contains one spreader, so the initial condition can be described as $I(0) = (N-1)/N \approx 1$, $S(0) = 1/N = 0$ and $R(0) = 0$. In the whole propagation process, stiflers are continuously rising with the increase of spreaders until the system only contains ignorants and stiflers. Then we define the final rumor size $R = \text{final}\{R(t)\} = 1 - I$, which is a variable to measure the extent of rumor propagation. Dividing Eq. (2) by Eq. (4), we can obtain

$$\frac{\mathrm{d}R(t)}{\mathrm{d}I(t)} = \frac{\mu\langle k\rangle S(t)[S(t)+R(t)] + \delta S(t)}{(-\lambda\alpha - \beta\lambda + \beta\lambda\alpha)\langle k\rangle I(t)S(t)},$$

that is,

$$\mathrm{d}R(t) = -\frac{\mu\,\mathrm{d}I(t)}{-\lambda\alpha - \beta\lambda + \beta\lambda\alpha} + \frac{\delta + \mu\langle k\rangle}{(-\lambda\alpha - \beta\lambda + \beta\lambda\alpha)\langle k\rangle I(t)}\mathrm{d}I(t). \tag{5}$$

We can integrate both sides of Eq. (5) for $R(t)$ and $I(t)$ from the original state to the stable state. Then we obtain the following transcendental equation:

$$R = 1 - \mathrm{e}^{-\varepsilon R}, \tag{6}$$

where

$$\varepsilon = \frac{(\lambda\alpha + \beta\lambda - \beta\lambda\alpha + \mu)\langle k\rangle}{\delta + \mu\langle k\rangle}. \tag{7}$$

The $R=0$ is always a trivial solution for Eq. (6). Besides, Eq. (6) has a non-zero solution only if $\varepsilon>1$. For $\delta\neq 0$, this condition can be satisfied easily if the following inequality is fulfilled:

$$\frac{\lambda}{\delta}>\frac{1}{\langle k\rangle(\alpha+\beta-\alpha\beta)}.$$

In a particular case, when $\delta=1$, we can obtain that the critical threshold of the modified SIR model on homogeneous networks is

$$\lambda_{\rm c}=\frac{1}{\langle k\rangle(\alpha+\beta-\alpha\beta)}. \tag{8}$$

According to the expression for the spreading threshold $\lambda_{\rm c}$, we can conclude that the spreading threshold depends on two parameters: α and β. In addition, the parameter α is decided by m and σ, so the spreading threshold is based on m, σ and β.

3.2. Heterogeneous modified SIR model

Next, we deal with the modified model on heterogeneous networks. Thus, we define the density of ignorants, spreaders and stiflers with k degree at the time t as $I_k(t)$, $S_k(t)$ and $R_k(t)$. According to the modified SIR model, we set up the following mean-field equations:

$$\frac{{\rm d}I_k(t)}{{\rm d}t}=(-\lambda\alpha-\beta\lambda+\beta\lambda\alpha)kI_k(t)\sum_{k'}S_{k'}(t)p(k'|k), \tag{9}$$

$$\begin{aligned}\frac{{\rm d}S_k(t)}{{\rm d}t}=&(\lambda\alpha+\beta\lambda-\beta\lambda\alpha)kI_k(t)\sum_{k'}S_{k'}(t)p(k'|k)\\&-\mu kS_k(t)\sum_{k'}[S_{k'}(t)+R_{k'}(t)]p(k'|k)-\delta S_k(t),\end{aligned} \tag{10}$$

$$\frac{{\rm d}R_k(t)}{{\rm d}t}=\mu kS_k(t)\sum_{k'}[S_{k'}(t)+R_{k'}(t)]p(k'|k)+\delta S_k(t). \tag{11}$$

On heterogeneous networks, the expression for the degree–degree correlations is $p(k'|k)=k'p(k')/\langle k\rangle=q(k')$. In the initial state of diffusion, we suppose that the density of the ignorant nodes $I_k(0)\approx 1$. Under such circumstances, Eq. (9) can be integrated directly to obtain $I_k(t)$,

$$I_k(t)={\rm e}^{(-\lambda\alpha-\beta\lambda+\beta\lambda\alpha)k\phi(t)}. \tag{12}$$

In Eq. (12), we introduce an auxiliary function as follows:

$$\phi(t)=\int_0^t\sum_k q(k)S_k(t'){\rm d}t'=\int_0^t\langle\langle S_k(t')\rangle\rangle{\rm d}t'.$$

Dealing with Eq. (10) by multiplying it with $q(k)$, summing over k and integrating the equation with respect to t, we obtain the following equation:

$$\begin{aligned}\frac{{\rm d}\phi(t)}{{\rm d}(t)}=&1-\langle\langle{\rm e}^{(-\lambda\alpha-\beta\lambda+\beta\lambda\alpha)k\phi(t)}\rangle\rangle\\&-\mu\int_0^t\langle\langle kS_k(t')\rangle\rangle[1-\langle\langle{\rm e}^{(-\lambda\alpha-\beta\lambda+\beta\lambda\alpha)k\phi(t')}\rangle\rangle]{\rm d}t'\\&-\delta\phi(t).\end{aligned}$$

When $t\to\infty$, ${\rm d}\phi(t)/{\rm d}t=0$, we set $\phi_\infty=\phi(\infty)$. From the above equation, we obtain

$$\begin{aligned}0=&1-{\rm e}^{(-\lambda\alpha-\beta\lambda+\beta\lambda\alpha)k\phi_\infty}\\&-\mu\int_0^\infty kS_k(t')\left[1-{\rm e}^{(-\lambda\alpha-\beta\lambda+\beta\lambda\alpha)k\phi(t')}\right]{\rm d}t'-\delta\phi_\infty.\end{aligned} \tag{13}$$

When $\mu=0$, we can obtain ϕ_∞ by solving Eq. (13). When $\mu\neq 0$, Eq. (13) can be solved to leading order into μ. By integrating Eq. (13) to zero order in μ, we get

$$\begin{aligned}S_k(t)=&1-{\rm e}^{(-\lambda\alpha-\beta\lambda+\beta\lambda\alpha)k\phi(t)}\\&-\delta\int_0^t S_k(t'){\rm d}t'+o(\mu).\end{aligned} \tag{14}$$

In order to deduce the expression of $\int_0^t S_k(t'){\rm d}t'$, we solve Eq. (14) by using the solution to the ODE

$$\begin{aligned}&\int_0^t S_k(t'){\rm d}t'\\=&\ {\rm e}^{-\delta t}\int_0^t\left[1-{\rm e}^{(-\lambda\alpha-\beta\lambda+\beta\lambda\alpha)k\phi(t)}\right]{\rm e}^{\delta t'}{\rm d}t'+o(\mu).\end{aligned} \tag{15}$$

Inserting Eq. (15) in Eq. (14), we obtain the expression of $S_k(t)$ as

$$\begin{aligned}S_k(t)=&1-{\rm e}^{(-\lambda\alpha-\beta\lambda+\beta\lambda\alpha)k\phi(t)}\\&-\delta\int_0^t\left[1-{\rm e}^{(-\lambda\alpha-\beta\lambda+\beta\lambda\alpha)k\phi(t')}\right]{\rm e}^{\delta(t'-t)}{\rm d}t'\\&+o(\mu).\end{aligned} \tag{16}$$

In order to obtain $S_k(t)$, we can expand Eq. (16) to the leading order in ϕ_∞ as

$$\begin{aligned}S_k(t)=&(\lambda\alpha+\beta\lambda-\beta\lambda\alpha)k\phi_\infty\left[f(t)-\delta\int_0^t f(t'){\rm e}^{\delta(t'-t)}{\rm d}t'\right]\\&+o(\mu)+o\left({\phi_\infty}^2\right).\end{aligned} \tag{17}$$

Afterwards, we solve Eq. (13) to get ϕ_∞. Insert Eq. (17) in Eq. (13) and expand the exponential to the relevant order in ϕ_∞, to yield ϕ_∞

$$\begin{aligned}0=&(\lambda\alpha+\beta\lambda-\beta\lambda\alpha)\langle\langle k\rangle\rangle\phi_\infty\\&-\mu\int_0^\infty\langle\langle k^2(\lambda\alpha+\beta\lambda-\beta\lambda\alpha)\phi_\infty\\&\times\left[f(t)-\delta\int_0^t f(t'){\rm e}^{\delta(t'-t)}{\rm d}t'\right]\rangle\rangle(\lambda\alpha+\beta\lambda-\beta\lambda\alpha)\\&\times\langle\langle k\rangle\rangle\phi_\infty f(t'){\rm d}t'-\frac{1}{2}(\lambda\alpha+\beta\lambda-\beta\lambda\alpha)^2\langle\langle k^2\rangle\rangle{\phi_\infty}^2\\&-\delta\phi_\infty+o\left({\phi_\infty}^3\right)+o\left(\mu^2\right).\end{aligned}$$

Consequently,

$$\begin{aligned}0=&\phi_\infty\Bigg[(\lambda\alpha+\beta\lambda-\beta\lambda\alpha)\langle\langle k\rangle\rangle-\delta\\&-(\lambda\alpha+\beta\lambda-\beta\lambda\alpha)^2\langle\langle k^2\rangle\rangle\phi_\infty\left(\frac{1}{2}+\mu\langle\langle k\rangle\rangle I\right)\Bigg],\end{aligned}$$

where

$$I=\int_0^{\infty}\left[f(t)-\delta\int_0^t f(t')\,\mathrm{e}^{\delta(t'-t)}\,\mathrm{d}t'\right]f(t')\,\mathrm{d}t',$$

that is a finite and positive-defined integral. Clearly, one solution of the above equation is $\phi_\infty=0$ and the other solution is

$$\phi_\infty=\frac{(\lambda\alpha+\beta\lambda-\beta\lambda\alpha)\langle\langle k\rangle\rangle-\delta}{(\lambda\alpha+\beta\lambda-\beta\lambda\alpha)^2\langle\langle k^2\rangle\rangle\left(\frac{1}{2}+\mu\langle\langle k\rangle\rangle I\right)},$$

which is a non-trivial solution. Noticing that $\langle\langle k\rangle\rangle=\langle k^2\rangle/\langle k\rangle, \langle\langle k^2\rangle\rangle=\langle k^3\rangle/\langle k\rangle$, so the threshold is

$$\lambda_{\mathrm{c}}'=\frac{\langle k\rangle\delta}{\langle k^2\rangle(\alpha+\beta-\alpha\beta)}. \tag{18}$$

As $R_k(\infty)=1-I_k(\infty)$, the expression of the final rumor size R is

$$\begin{aligned}R&=\sum_k P(k)R_k(\infty)=\sum_k P(k)\left[1-I_k(\infty)\right]\\&=\sum_k P(k)\left[1-\mathrm{e}^{(-\lambda\alpha-\beta\lambda+\beta\lambda\alpha)k\phi_\infty}\right].\end{aligned}$$

4. Immunization strategies

How to control the contagion of the rumor is a significant issue in our daily life. Accordingly, immunization strategies have been introduced to deal with the dissemination of rumors. In this part, we will carry out several strategies to reduce the influence of rumor diffusion. Based on the characteristic of degree fluctuation in heterogeneous networks is distinct and more complex, which is similar to the real-world network, so we focus on our investigation on heterogeneous networks. We perform random immunization, acquaintance immunization, targeted immunization, and active immunization. The effectiveness of different controls will be verified in rumor propagation, and a parallel comparison among different controls will be given.

4.1. Random immunization

In heterogeneous networks, random immunization is a common strategy to be considered. Firstly, we set the applicable immunization rate p $(0<p<1)$. To some extent, the random immunization strategy can decrease the spreading rate λ by a factor $1-p$. Thus Eqs. (9)–(11) become

$$\begin{aligned}\frac{\mathrm{d}I_k(t)}{\mathrm{d}t}&=-\lambda(1-p)(\alpha+\beta-\beta\alpha)kI_k(t)\sum_{k'}S_{k'}(t)p(k'|k),\\\frac{\mathrm{d}S_k(t)}{\mathrm{d}t}&=\lambda(1-p)(\alpha+\beta-\beta\alpha)kI_k(t)\sum_{k'}S_{k'}(t)p(k'|k)\\&\quad-\mu kS_k(t)\sum_{k'}[S_{k'}(t)+R_{k'}(t)]p(k'|k)-\delta S_k(t),\\\frac{\mathrm{d}R_k(t)}{\mathrm{d}t}&=\mu kS_k(t)\sum_{k'}[S_{k'}(t)+R_{k'}(t)]p(k'|k)+\delta S_k(t).\end{aligned}$$

On the basis of the above derivation method of ϕ_∞, we can get the auxiliary function under random immunization

$$\phi_{\infty 1}=\frac{\lambda(1-p)(\alpha+\beta-\beta\alpha)\langle\langle k\rangle\rangle-\delta}{[\lambda(1-p)(\alpha+\beta-\beta\alpha)]^2\langle\langle k^2\rangle\rangle\left(\frac{1}{2}+\mu\langle\langle k\rangle\rangle I\right)}. \tag{19}$$

Thus, the spreading threshold is

$$\overline{\lambda_{\mathrm{c}}'}=\frac{\delta\langle k\rangle}{(1-p)\langle k^2\rangle(\alpha+\beta-\alpha\beta)}=\frac{1}{1-p}\lambda_{\mathrm{c}}'>\lambda_{\mathrm{c}}'.$$

4.2. Targeted immunization

Random immunization regards every node in the system with the same significance, whereas nodes with different degrees, clustering coefficients,[45] betweenness centralities,[46] and degree centralities[47] exert different influences in networks. Hence, in heterogeneous networks, many immunizations have been discussed. Targeted immunization is an effective method to control rumor diffusion. In the first place, we set an upper threshold k_{T}. If a node with degree k is greater than k_{T}, it will be immunized. Hence, we define the immunization rate ε_k as follows:

$$\varepsilon_k=\begin{cases}1, & k>k_{\mathrm{T}},\\ c, & k=k_{\mathrm{T}},\\ 0, & k<k_{\mathrm{T}},\end{cases}$$

where $c\in(0,1)$ and the average immunization rate $\overline{\varepsilon}=\sum_k p(k)\varepsilon_k$. Consequently, the mean-field equations become

$$\begin{aligned}\frac{\mathrm{d}I_k(t)}{\mathrm{d}t}&=-\lambda(1-\varepsilon_k)(\alpha+\beta-\beta\alpha)kI_k(t)\sum_{k'}S_{k'}(t)p(k'|k),\\\frac{\mathrm{d}S_k(t)}{\mathrm{d}t}&=\lambda(1-\varepsilon_k)(\alpha+\beta-\beta\alpha)kI_k(t)\sum_{k'}S_{k'}(t)p(k'|k)\\&\quad-\mu kS_k(t)\sum_{k'}[S_{k'}(t)+R_{k'}(t)]p(k'|k)-\delta S_k(t),\\\frac{\mathrm{d}R_k(t)}{\mathrm{d}t}&=\mu kS_k(t)\sum_{k'}[S_{k'}(t)+R_{k'}(t)]p(k'|k)+\delta S_k(t).\end{aligned}$$

This leads to

$$\phi_{\infty 2}=\frac{\lambda(\alpha+\beta-\beta\alpha)\langle\langle(1-\varepsilon_k)k\rangle\rangle-\delta}{[\lambda(\alpha+\beta-\beta\alpha)]^2\langle\langle(1-\varepsilon_k)k^2\rangle\rangle\left(\frac{1}{2}+\mu\langle\langle k\rangle\rangle I\right)}.$$

Therefore, the threshold under the targeted immunization is

$$\begin{aligned}\lambda_{\mathrm{c}2}&=\frac{\delta}{\langle\langle k(1-\varepsilon_k)\rangle\rangle(\alpha+\beta-\alpha\beta)}\\&=\frac{1}{1-\frac{\langle k^2\varepsilon_k^2\rangle\langle k\rangle}{\langle k\varepsilon_k\rangle\langle k^2\rangle}}\lambda_{\mathrm{c}}'=\frac{1}{1-\frac{\langle\langle k\varepsilon_k\rangle\rangle}{\langle\langle k\rangle\rangle}}\lambda_{\mathrm{c}}'>\lambda_{\mathrm{c}}'.\end{aligned}$$

4.3. Acquaintance immunization

The targeted immunization, while effective, requires us to set an upper threshold based on global knowledge, rendering it impractical on networks. To get rid of this defect, we perform the acquaintance immunization strategy, requiring no knowledge of degrees or any other global conditions. As same as random immunization, the first step of acquaintance immunization is to choose pN nodes at random. Next,

we seek a random acquaintance with whom they are in contact. Then, these acquaintances will be immunized rather than the initially chosen nodes. Consequently, the nodes with k degree in heterogeneous networks are immunized by the probability $p_k = pN \cdot kp(k)/N\langle k\rangle = pkp(k)/\langle k\rangle$. By considering the above control strategy, the mean-field equations become

$$\begin{aligned}
\frac{\mathrm{d}I_k(t)}{\mathrm{d}t} &= -\lambda(1-p_k)(\alpha+\beta-\beta\alpha)kI_k(t)\sum_{k'}S_{k'}(t)p(k'|k),\\
\frac{\mathrm{d}S_k(t)}{\mathrm{d}t} &= \lambda(1-p_k)(\alpha+\beta-\beta\alpha)kI_k(t)\sum_{k'}S_{k'}(t)p(k'|k)\\
&\quad -\mu kS_k(t)\sum_{k'}[S_{k'}(t)+R_{k'}(t)]p(k'|k)-\delta S_k(t),\\
\frac{\mathrm{d}R_k(t)}{\mathrm{d}t} &= \mu kS_k(t)\sum_{k'}[S_{k'}(t)+R_{k'}(t)]p(k'|k)+\delta S_k(t).
\end{aligned}$$

The auxiliary function $\phi_{\infty 3}$ is

$$\phi_{\infty 3} = \frac{\lambda(\alpha+\beta-\beta\alpha)\langle\langle(1-p_k)k\rangle\rangle-\delta}{[\lambda(\alpha+\beta-\beta\alpha)]^2\langle\langle(1-p_k)k^2\rangle\rangle\left(\frac{1}{2}+\mu\langle\langle k\rangle\rangle I\right)}.$$

Substituting $p_k = pkp(k)/\langle k\rangle$ into the auxiliary function, we obtain

$$\begin{aligned}
\lambda_{c3} &= \frac{\delta}{\langle\langle k(1-p_k)\rangle\rangle(\alpha+\beta-\alpha\beta)}\\
&= \frac{1}{1-\frac{\langle k^2{p_k}^2\rangle\langle k\rangle}{\langle kp_k\rangle\langle k^2\rangle}}\lambda_c' = \frac{1}{1-\frac{\langle\langle kp_k\rangle\rangle}{\langle\langle k\rangle\rangle}}\lambda_c' > \lambda_c'.
\end{aligned}$$

4.4. Active immunization

Despite reducing the immunization threshold, to some extent,acquaintance control might immunize the neighbor nodes which play a minor role in networks or have few connected nodes. In social networks, since highly connected nodes are more inclined to transmit the rumor, it is absolutely essential to control neighbor nodes with a large degree rather than randomly select, which is advantageous to control rumors. Hence, we perform the active immunization to verify its effectiveness and validity. The core point of active immunization is to randomly choose $p\%$ nodes and immunize all neighbor nodes with degree $k > \kappa$. The expression of immunization propagation is

$$\gamma_k = \begin{cases} 1, & k > \kappa,\\ c, & k = \kappa,\\ 0, & k < \kappa, \end{cases}$$

where $c \in (0,1)$ and the average immunization rate $\overline{\gamma_k} = \sum_k p(k)\gamma_k$. Consequently, the mean-field equations become

$$\begin{aligned}
\frac{\mathrm{d}I_k(t)}{\mathrm{d}t} &= -\lambda(\alpha+\beta-\beta\alpha)kI_k(t)\sum_{k'}S_{k'}(t)p(k'|k),\\
\frac{\mathrm{d}S_k(t)}{\mathrm{d}t} &= \lambda(\alpha+\beta-\beta\alpha)kI_k(t)\sum_{k'}S_{k'}(t)p(k'|k)\\
&\quad -\mu kS_k(t)\sum_{k'}[S_{k'}(t)+R_{k'}(t)]p(k'|k)-(\delta+\overline{\gamma_k})S_k(t),\\
\frac{\mathrm{d}R_k(t)}{\mathrm{d}t} &= \mu kS_k(t)\sum_{k'}[S_{k'}(t)+R_{k'}(t)]p(k'|k)+(\delta+\overline{\gamma_k})S_k(t).
\end{aligned}$$

The auxiliary function $\phi_{\infty 4}$ is

$$\phi_{\infty 4} = \frac{\lambda(\alpha+\beta-\beta\alpha)\langle\langle k\rangle\rangle-(\delta+\overline{\gamma_k})}{[\lambda(\alpha+\beta-\beta\alpha)]^2\langle\langle k^2\rangle\rangle\left(\frac{1}{2}+\mu\langle\langle k\rangle\rangle I\right)}.$$

Substituting $\overline{\gamma_k} = \sum_k p(k)\gamma_k$ into the auxiliary function, we obtain the immunization threshold as

$$\begin{aligned}
\lambda_{c4} &= \frac{\delta+\overline{\gamma_k}}{\langle\langle k\rangle\rangle(\alpha+\beta-\alpha\beta)} = \frac{\delta\langle k\rangle+\langle k\gamma_k\rangle}{(\alpha+\beta-\alpha\beta)\langle k^2\rangle}\\
&= \lambda_c' + \frac{\langle k\gamma_k\rangle}{(\alpha+\beta-\alpha\beta)\langle k^2\rangle} > \lambda_c'.
\end{aligned}$$

From the above theoretical derivation, immunization thresholds under four different immunization strategies are bigger than the spreading threshold without any controls. Therefore, we can conclude that the above four kinds of controls can effectively reduce the impact of rumors.

5. Simulation results

In this subsection, we conduct several simulations to verify the theoretical results achieved on the front part and test the sensitivity of relevant parameters. Two representative networks, WS network[48] and BA scale-free network,[49] are discussed to perform the rumor diffusion process. Additionally, we apply the modified model to a real-world social network, the Facebook network. The size of WS network is $N = 5000$, the average degree is $\langle k\rangle = 6$ and the rewiring probability is $p = 0.5$. For BA network, the growth of edges and the initial number of nodes are set as 6, respectively. Meanwhile, BA network size and average degree are the same as those on WS network. The basic settings of Facebook network are as follows: the size of the network is $N = 4039$; the number of edges is 88234 and the average degree is nearly 43.69. The schematic diagram of the topology is shown in Fig. 3. To evidently exhibit the feature of networks, the degree distributions of three networks are shown in Fig. 4.

It is visual to see from Figs. 3 and 4, the degree fluctuation of WS network is not evident. In contrast, the degree distribution of BA scale-free network approximately follows the power-law distribution, and the maximum and minimum values of degree have a significant disparity.[50] Identically, the difference of degree is quite distinct in Facebook network and there are more hub nodes than BA network. To some extent, WS network can represent a real-world network which has a small diameter. BA scale-free network is chosen as a suitable real-world network which has the scale-free characteristic. Furthermore, we set $\delta = 1$, $\mu = 0.5$ and $b = 6$. The optimal value of b is 6 which is obtained through many tests. To avoid randomness, all the following simulations are performed by choosing a randomly initial spreader and the corresponding results are averaged over 50 times with different rumormongers.

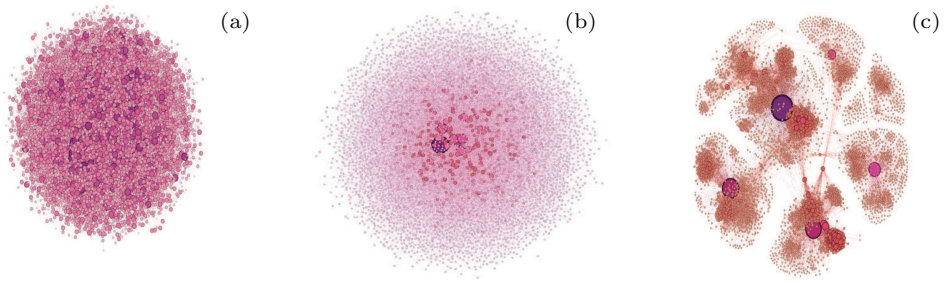


Fig. 3. Nodes that have higher degrees are larger and darker in area. (a) WS network topology. (b) BA scale-free network topology. (c) Facebook network topology.

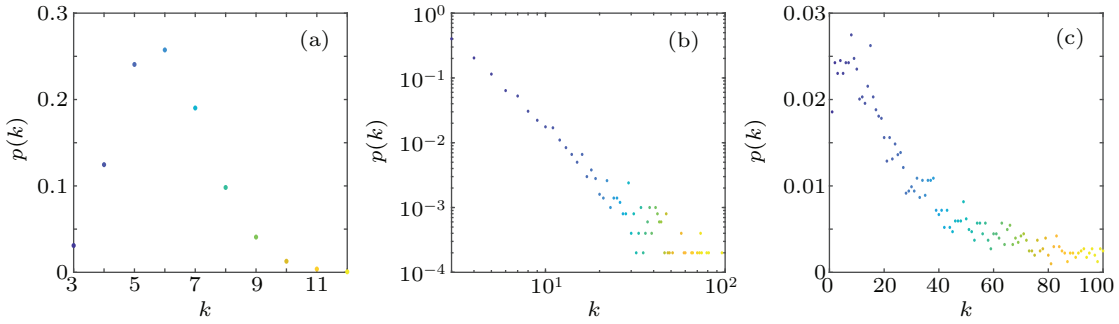


Fig. 4. The degree distribution function $p(k)$ of three networks. (a) WS network. (b) BA scale-free network. (c) Facebook network topology.

5.1. The evolution of different nodes

To begin with, we research the impact of the network topology on the rumor diffusion process and the density variation of different nodes. Figure 5 vividly reflects the theoretical value of mean-field equations on the homogeneous network, the course of rumor diffusion on artificial networks and a real-world social network.

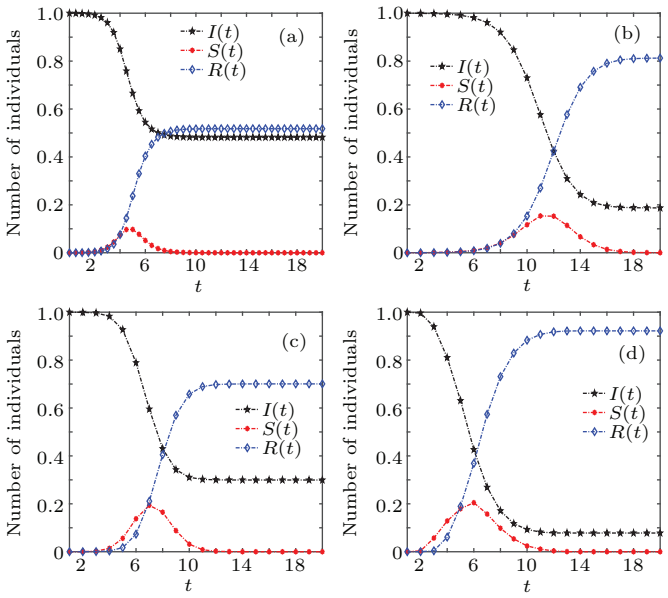


Fig. 5. The evolution of rumor propagation with $\lambda = \beta = \sigma = 0.5$, $m = 2/15$: (a) the theoretical value of the modified model in homogeneous network, (b) the modified SIR model in WS network, (c) the modified SIR model in BA scale-free network, (d) the modified SIR model in Facebook network.

In Fig. 5(a), the theoretical value of the modified model has been presented. Clearly, the density of spreaders in the early scenario grows up until it reaches peak value. The decrease of spreaders from its peak value to zero means the extinction courses of the rumor diffusion. Finally, there are only stiflers and ignorants that exist in networks. In this course, the density of stiflers in each step continuously increases until it reaches a steady state. The trend of theoretical values on the homogeneous network is basically identical with the WS network.

Besides, it is clear to see that the ultimate rumor size on Facebook is the largest. The WS network comes second and BA network has the smallest final rumor size. Nevertheless, the time rumor required to reach the steady-state and its peak value on Facebook is shorter than BA network and WS network. Moreover, we obtain that the final size of rumor on WS network is more considerable than BA network, whereas the spreading speed on BA network is faster than WS network. These conclusions are consistent with results on the general BA network and WS network.[5]

The significant difference in the spreading rate among the three networks is due to the network topology that some highly connected nodes on BA network and Facebook network contribute to more neighbor nodes getting the rumor easily and disseminating the rumor to others efficiently. To some extent, hub nodes greatly accelerate the process of rumor spreading. However, once hub nodes turn into stiflers, they also impede further propagation. Especially, Facebook has the most highly connected nodes than two other networks. If the few hub nodes in Facebook start to spread the rumor, they will lead to the rumor spreading through the whole network for a short time while the number of nodes involved in the process

of spreading in WS and BA networks is fewer than Facebook at the same time. Therefore, the rumor diffuses the fastest and sets out to be on the wane at the earliest, and finally become extinct in Facebook network.

5.2. The links between spreading rate and final rumor size for different parameters

In this subsection, we are trying to seek links between the spreading rate and the final rumor size R for different parameters. Besides, we will also test the sensitivity of the relevant parameters. Studies of percolation theory [51] on broad-scale networks show that if the probability of spreading probability λ is small, which is less than the outbreak threshold, the spread of the rumor will stop. In contrast, if the probability of spreading probability is greater than the outbreak threshold, the rumor will spread all over the network. In the process of rumor diffusion, when the values of the final rumor size visibly beyond the original value, the rumor will break out in the system and the corresponding value of spreading rate is the spreading threshold.

Firstly, we investigate the effect of different β values on rumors on three networks, where we set $\sigma = 0.5$, $m = 0.13$ and $\beta = 0$, 0.4, 0.8 and 1. In Fig. 6, the final size of rumor R increases as the spreading rate λ increases on three networks. Furthermore, the parameter β has an evident influence on the spreading threshold on WS and BA networks as well as no apparent difference on Facebook network. Figure 6(a) presents the critical thresholds $\lambda_c = 0.24$, 0.21, 0.19 and 0.15 (as the black arrows denoted in the figure) in WS network, which is basically in accord with the theoretical derivation from Eq. (8) ($\lambda_c = 0.24$, 0.2, 0.17 and 0.16, $\langle k \rangle = 6$). Figure 6(b) mirrors the critical thresholds $\lambda_c = 0.06$, 0.07, 0.08 and 0.12 in BA network, which is nearly consistent with the theoretical derivation from Eq. (18) ($\lambda_c = 0.083$, 0.088, 0.102 and 0.12, $\langle k^2 \rangle = 71.788$). Figure 6(c) depicts the critical thresholds tend to zero in Facebook network, which conforms to the theoretical derivation from Eq. (18) ($\lambda_c = 0.013$, 0.011, 0.01 and 0.009, $\langle k \rangle = 43.69$, $\langle k^2 \rangle = 4656$).

It is clear to see that the critical threshold λ_c decreases with the increase of β on WS and BA network. It might be concluded by the fact that the higher value of β leads to untrusted and unrelated nodes spreading rumors at a high level, so the whole transmission rate increases which causes the critical threshold λ_c to decrease. For Facebook network, when the rumor develops in the early scenario, the whole system remains unaware of its existence whereas hub nodes have already propagated the rumor to many ignorants within a short time. Hence, some parameters have a trifling impact on the critical threshold and the final size of rumor in Facebook network on account of the rumor erupting completely off-guard. Moreover, when λ is close to 1, the different values of β have no apparent effects on the final rumor size on WS and Facebook networks, whereas the change is very evident on BA scale-free network.

In Fig. 7, R is described as a function of λ with four different values of the correlation coefficient σ on three networks, where we set $\beta = 0.5$, $m = 0.13$ and $\sigma = 0$, 0.3, 0.6 and 0.9. Figure 7(a) presents the critical thresholds $\lambda_c = 0.3$, 0.27, 0.19 and 0.17 in WS network, which is basically in accord with theoretical results from Eq. (8) ($\lambda_c = 0.3$, 0.23, 0.184 and 0.169). Figure 7(b) mirrors the critical thresholds $\lambda_c = 0.12$, 0.1, 0.08 and 0.06 in BA network, which is nearly consistent with the theoretical derivation from Eq. (18) ($\lambda_c = 0.15$, 0.11, 0.09 and 0.08). Figure 7(c) depicts the critical thresholds tend to zero in Facebook network, which conforms to the theoretical derivation from Eq. (18) ($\lambda_c = 0.017$, 0.013, 0.01 and 0.009).

Obviously, the final size of rumor R increases as the spreading rate λ increases until reaching a steady state on three networks. From the above pictures, in Facebook, the correlation coefficient σ takes no important role in the spreading threshold, while in the WS and BA networks, with the increase of σ, the final rumor size R increases and the the critical threshold λ_c decreases. The differences exist in three networks primarily in respect that the more relevant the rumor to life, the more people involved. In fact, given a fixed m, spreaders are more likely to contact ignorants involved in rumors to spread a rumor with a higher spreading rate which makes the combination of trust mechanism and correlation mechanism plays a crucial role in spreading rumors. On account of the higher transmission rate and more people involved in rumor spreading, the final rumor size increases.

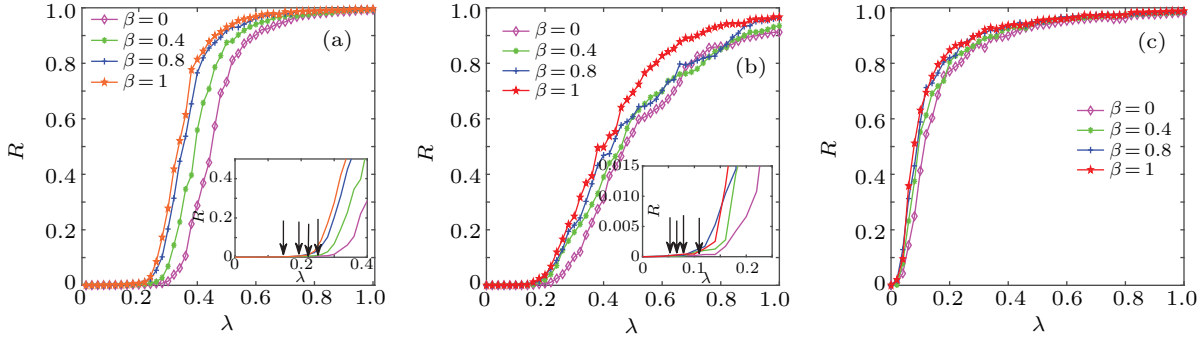


Fig. 6. The final size of the rumor is shown as a function of the spreading rate λ for different values of β. (a) The modified SIR model in WS network. (b) The modified SIR model in BA scale-free network. (c) The modified SIR model in Facebook network.

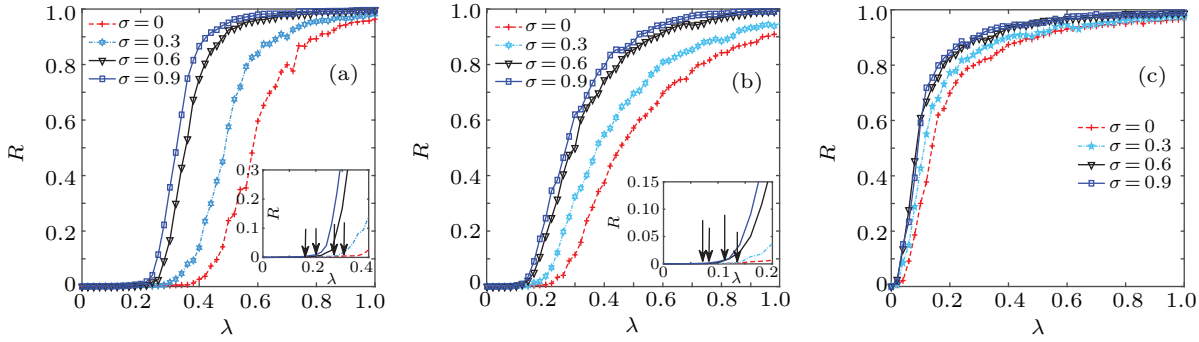


Fig. 7. The final size of the rumor is shown as a function of the spreading rate λ for several values of σ. (a) The modified SIR model in WS network. (b) The modified SIR model in BA scale-free network. (c) The modified SIR model in Facebook network.

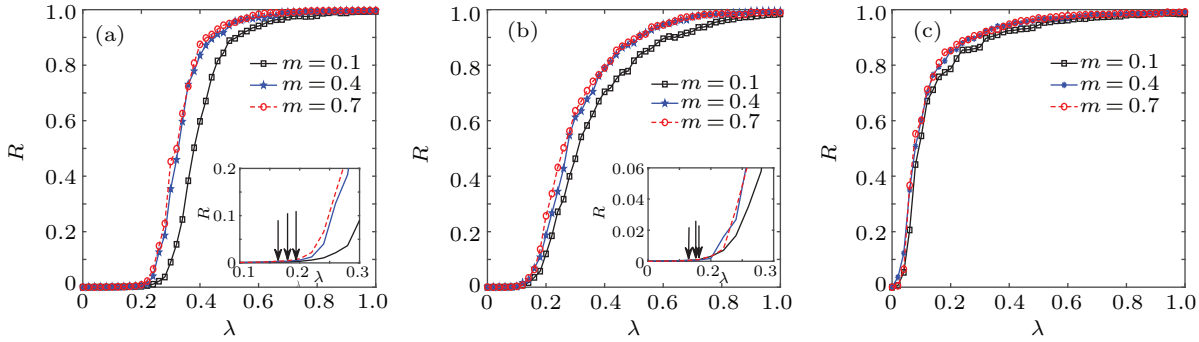


Fig. 8. The final size of the rumor is shown as a function of the spreading rate λ for several values of σ. (a) The modified SIR model in WS network. (b) The modified SIR model in BA scale-free network. (c) The modified SIR model in Facebook network.

Figure 8 presents the same rising tendency between λ and R with the variation of parameter m on three networks. Figure 8(a) presents the critical thresholds $\lambda_c = 0.19$, 0.18 and 0.17 in WS network, which is basically in accord with the theoretical derivation from Eq. (8) ($\lambda_c = 0.19$, 0.17 and 0.16). Figure 8(b) mirrors the critical thresholds $\lambda_c = 0.09$, 0.08 and 0.06 in BA network, which is nearly consistent with the theoretical derivation from Eq. (18) ($\lambda_c = 0.09$, 0.086 and 0.084). Figure 8(c) depicts the critical thresholds tend to zero in Facebook network, which conforms to the theoretical derivation from Eq. (18) ($\lambda_c = 0.01$, 0.0097 and 0.0094).

Comparing three subgraphs, we can obtain some similarities and differences. Firstly, the most apparent point is that the three subgraphs have the same escalating trend that if there is an increase in the spreading rate, the final size of rumor R becomes greater on three networks. Secondly, WS and BA networks have their own spreading threshold λ_c, whereas λ_c and the final rumor size R in WS network are more extensive than BA scale-free network, mainly because hub nodes exist in the BA scale-free network. Besides, the degrees of hub nodes in Facebook network largely outweigh BA network, contributing to the rumor booming in the early scenario. Hence, the critical threshold in Facebook network tends to zero on account of the bigger hub nodes. Thirdly, the higher the trusted proportion m, the higher the final rumor size R. When λ is close to 1, with the different values of the trusted proportion m, there is a marked change in the final rumor size R in BA scale-free network, yet the change in WS and Facebook networks is very slight. The above phenomenon is virtually since if a spreader has more intimate friends, he will be inclined to propagate a rumor to intimate friends with a higher spreading rate. Thus, the rising number of ignorants turn to spreaders, leading to more stiflers in the system.

5.3. Correlation mechanism exerts influence on different nodes

Next, we simulate the evolution condition of the stifler nodes and spreader nodes with the change of time t for different values of σ on three networks, where we set $\lambda = 0.5$, $\beta = 0.5$, and $m = 0.13$. When $\sigma = 0$, it means that the rumor is not related to our life, so only trusted people propagate the rumor at a high spreading rate and untrusted people and unrelated people spread the rumor at a low spreading rate. In this case, the system only considers the trust mechanism that is in accord with the previous model.[29] When $\sigma = 1$, the rumor is inextricably linked to our life, so all neighbor nodes propagate the rumor at a high spreading rate.

As is shown in Fig. 9, the utilization of the two mechanisms increases the final rumor size and minimizes the time that the system reaches a steady state on three networks. That is to say, the combination of two mechanisms increases the whole diffusion speed, making the rumor more challenging to control than without the correlation mechanism. When $\sigma = 1$, the density of the final rumor size reaches 1 on three networks, which means only the stifler node exists in networks.

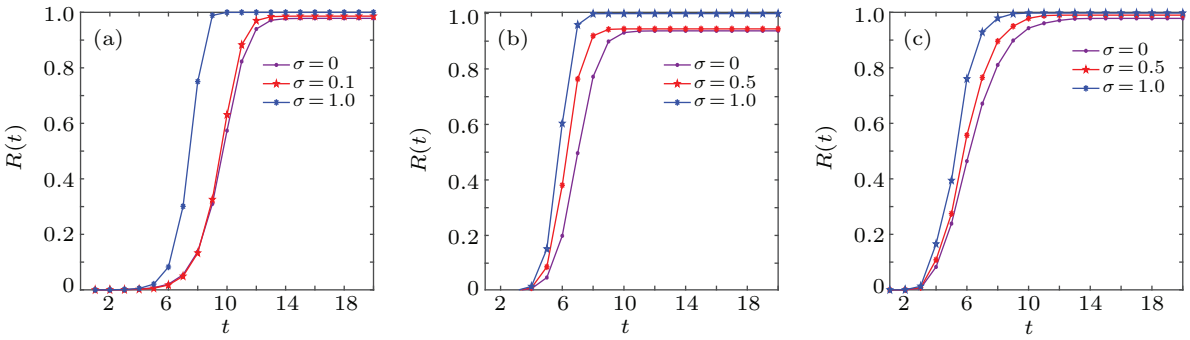


Fig. 9. The evolution condition of stifler nodes $R(t)$ with the change of time t for different values of σ. (a) The modified SIR model in WS network. (b) The modified SIR model in BA scale-free network. (c) The modified SIR model in Facebook network.

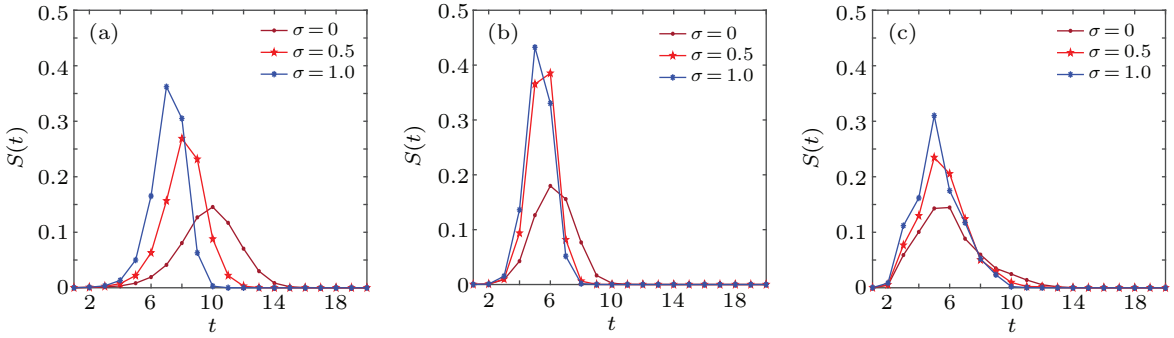


Fig. 10. The evolution condition of spreader nodes $S(t)$ with the change of time t for different values of σ. (a) The modified SIR model in WS network. (b) The modified SIR model in BA scale-free network. (c) The modified SIR model in Facebook network.

In Fig. 10, the most crucial point is the peak value of spreaders, which measures the maximum rumor influence. Comparing a system including two mechanisms with only the trust mechanism, the duration of rumor spreading becomes shorter, and the peak value of $S(t)$ grows up rapidly. To be more specific, the bigger the correlation coefficient, the larger the peak value of the spreader. If we pay enough attention to the rumor before the time threshold, the rumor will not spread all over the system.

5.4. Immunization strategies

Realizing vicious rumors have enormous damage to our daily life, we should adopt effective measures to impede rumor diffusion. Based on the modified SIR model, we perform four immunization strategies and compare the effectiveness of different immunization strategies in BA scale-free network.

5.4.1. The effectiveness of different immunization strategies on the modified SIR model

Figure 11 depicts densities of the spreader versus time changing under different immune proportions or upper thresholds in BA network. From the above four subgraphs, we can see that all four different immunization strategies effectively decrease the peak values of the spreader. For random immunization strategy, with the increase of immune proportions that more ignorants are immunized, spreaders take more time to get the peak value, and fewer spreaders exist in the system. Then, we carry out acquaintance immunization by setting the

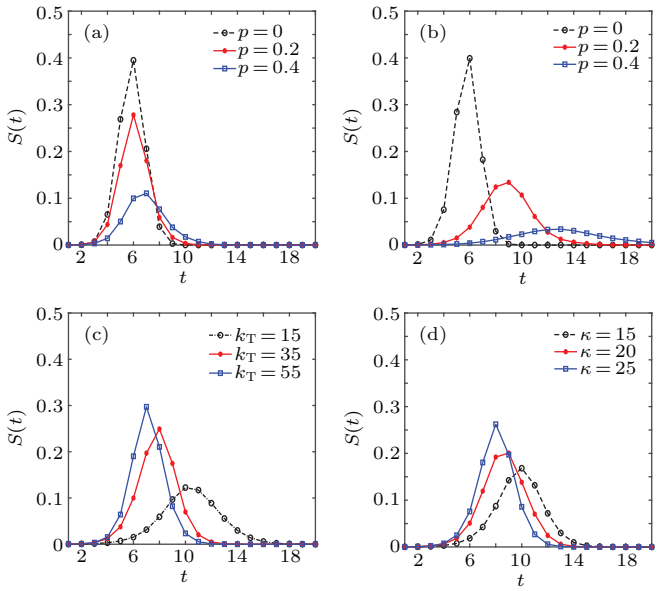


Fig. 11. Densities of spreader versus time varying over different immunization strategies with $\lambda = 0.9$, $\beta = 0.7$, $m = 0.13$, $\sigma = 0.5$, $\mu = 0.5$: (a) random immunization, (b) acquaintance immunization, (c) targeted immunization, (d) active immunization, (d) active immunization.

identical immune proportions and other related parameters as random immunization. It can be seen from Fig. 11(b), when $p = 0$, the modified SIR without immunization strategy has the maximum rumor influence. With the increase of immune proportions, acquaintance immunization plays an increasing role in rumor propagation and finally leads to the smaller scale of spreaders. Next, we conduct two controls, namely, targeted immunization and active immunization, which need to set an

upper threshold, respectively. Comparing the principle of targeted immunization with active immunization, the restraint of targeted immunization is more inclusive. In Fig. 11(c), with the decrease of the upper threshold, more nodes are immunized, leading to the maximum rumor influence decrease. In other words, the lower the upper threshold, the smaller the peak value of spreaders. Active immunization with two selection steps is more complex than targeted immunization, whereas it requires no knowledge of global conditions. In Fig. 11(d), it is clear to see that with the decrease of the upper threshold, the density of the spreader's peak value decreases. The tendency is since the higher the degree, the fewer the corresponding nodes in the system. Therefore, the smaller upper threshold will contribute to a better way to control rumors.

5.4.2. The impact of different immunization strategies on the critical threshold and the final rumor size

Figure 12 clearly presents the influence of immunization strategies on the critical threshold and the final rumor size. Under no immunization control, the source of the stifler only depends on the spreader. In the context of immunization controls, the increase of the stifler comes from the spreader in the process of diffusion and the immunized node which is selected in the initial state by different methods. Therefore, the outbreak of the rumor is decided by the increase of the final rumor size. In Figs. 12(a) and 12(b), with the increase of immune proportion, the values of the spreading threshold increase, whereas the final rumor size decrease. The more nodes are immunized in the initial state, the greater probability the spreader and ignorant contact the stifler. Afterward, the system will have a better capability to defend the rumor.

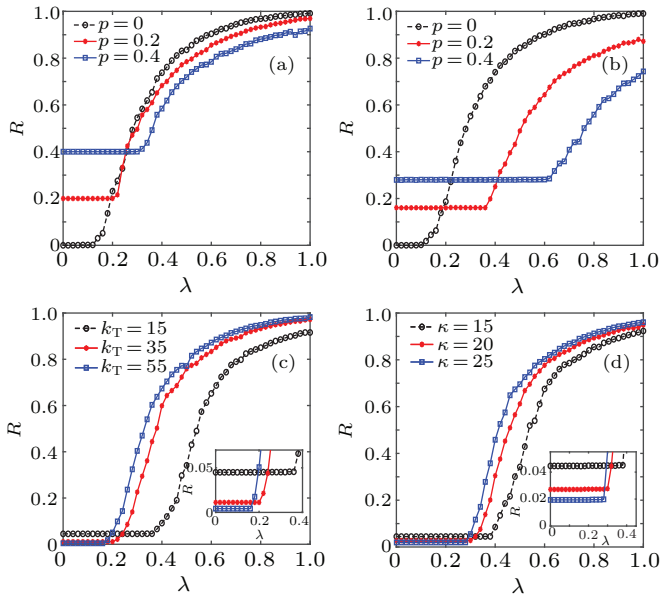


Fig. 12. The final size of the rumor is shown as a function of the spreading rate λ for different immunization strategies with $\lambda=0.9$, $\beta=0.7$, $m=0.13$, $\sigma=0.5$, $\mu=0.5$: (a) random immunization, (b) acquaintance immunization, (c) targeted immunization, (d) active immunization, (d) active immunization.

Hence, the spreading threshold needs to be large enough to make the rumor break out in the system. Besides, there are fewer spreaders involved in the rumor, leading to the smaller final rumor size. Figures 12(c) and 12(d) depict the targeted immunization and the active immunization, respectively. In social networks, the number of hub nodes is relatively scarce. The bigger the upper threshold we choose, the fewer nodes are immunized. Then, there are fewer stiflers at the beginning, contributing to the network becoming an immunologically defenseless system. As a result, more and more spreaders take part in spreading rumors which leads to the increase of the final rumor size and decrease of spreading threshold.

5.4.3. The impact of the trust mechanism on different immunization strategies

In Fig. 13, $S(t)$ is plotted as a function of t with three different values of the trusted proportions under different immunization controls. From the above four subgraphs, it is clear to see the densities of the spreader increase firstly and then decrease. Moreover, the peak value of the spreader decreases as the trust proportion decrease under different controls.

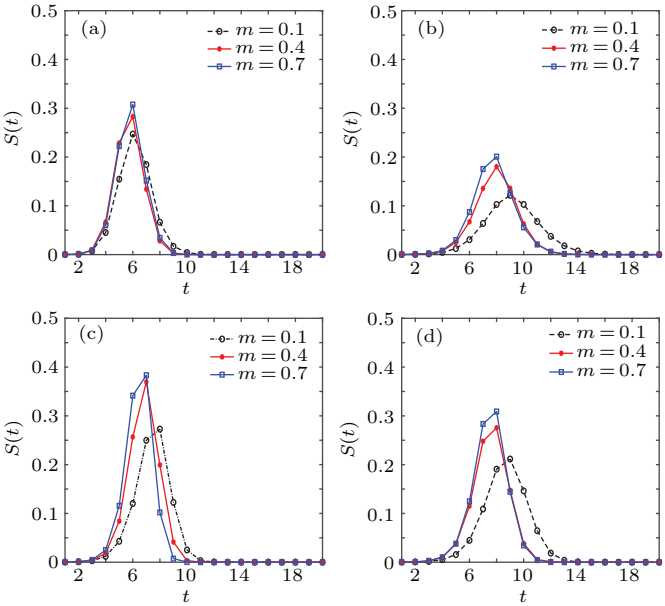


Fig. 13. Densities of spreader versus time varying for different values of m under different immunization strategies with $\lambda=0.9$, $\beta=0.7$, $\sigma=0.5$, $\mu=0.5$, $p=0.2$, $k_T=35$, $\kappa=20$: (a) random immunization, (b) acquaintance immunization, (c) targeted immunization, (d) active immunization, (d) active immunization.

To the above four strategies, when immunization parameters are decided in the initial scenario, the immunized node is fixed which is not affected by the trust proportion. The variation of m only impacts the process of rumor propagation. Under the circumstance of nodes being immunized, with the increase of m, more nodes will spread the rumor to their trust friends with a higher spreading rate which further facilitates the outbreak of the rumor and hasten the terminal of the rumor.

5.4.4. The impact of the correlation mechanism on different immunization strategies

Next, $S(t)$ is plotted as a function of t with three different values of the correlation coefficient under different immunization controls. In Fig. 14, it is unambiguous to find that the trend of the spreader is virtually the same as Fig. 13. Besides, the peak value of the spreader decreases as the correlation coefficient decreases under different controls. To some extent, the reason for the influence of the correlation mechanism on the four strategies is as same as the trust mechanism. Specifically speaking, two mechanisms do not affect the initial immunized nodes, but impact the course of propagation. When the immunized parameters are fixed, with the increase of σ, the rumor is more relevant to our life, which results in more nodes taking part in spreading the rumor. Therefore, the introduction of the correlation mechanism weakens the function of immunization strategies.

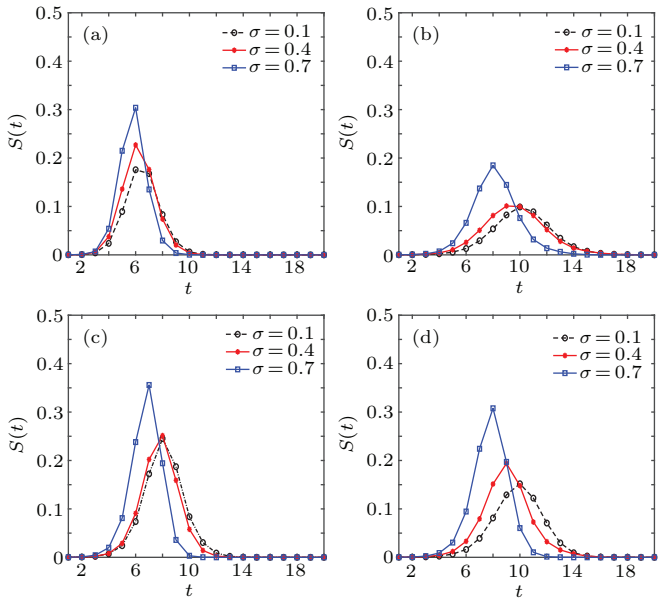


Fig. 14. Densities of spreader versus time varying for different values of σ under different immunization strategies with $\lambda = 0.9$, $\beta = 0.7$, $m = 0.13$, $\mu = 0.5$, $p = 0.2$, $k_{\mathrm{T}} = 35$, $\kappa = 20$: (a) random immunization, (b) acquaintance immunization, (c) targeted immunization, (d) active immunization, (d) active immunization.

5.4.5. A parallel comparison of different immunization strategies

Next, we contrast the effectiveness of different immunizations in BA network. Figure 15 reflects that the density of spreader nodes changes with time under no immunization, random immunization, targeted immunization, acquaintance immunization, and active immunization. Firstly, comparing with no immunization, the peak values of spreaders under four different immunization strategies decrease, which means the above strategies effectively control rumor propagation. Secondly, the time required for the spreader to reach the peak value under four immunization controls is extended, which gives us more response time to control rumors. Thirdly, comparing four kinds of strategies, we can conclude that the effectiveness of immunization controls is in this order: targeted immunization first, active immunization second, acquaintance immunization third, and random immunization fourth.

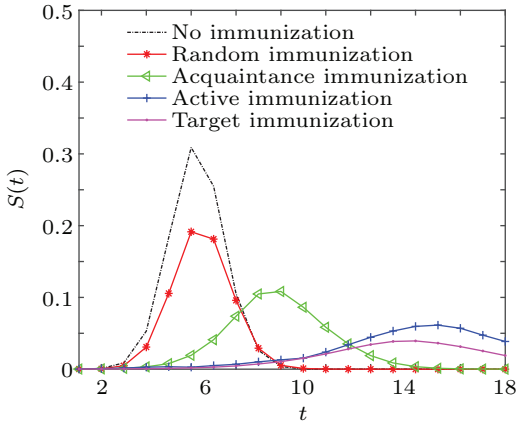


Fig. 15. Densities of spreader versus time varying under different immunization strategies in BA network with $\lambda = 0.9$, $\beta = 0.7$, $m = 0.13$, $\sigma = 0.5$.

6. Conclusion

In this paper, an improved SIR model is put forward, in which the combination of two mechanisms by the Ridenour model reflects the psychological factors of individuals when in contact with rumors. Then we set up the mean-field equations on homogeneous networks and heterogeneous networks. Next, experiments are performed to validate the effectiveness and preciseness of the modified model on three networks. It reveals that two mechanisms increase the final rumor size on three networksand reduce the spreading threshold on WS and BA networks. In addition, the new model cuts down the duration of the rumor, which gives us less time to adopt measures to impede the rumor. Besides, four immunization controls are investigated. The above four controls increase the spreading threshold and decrease the final rumor size. Moreover, the introduction of trust and correlation mechanisms weakens the function of immunization strategies. To be more specific, the random immunization is better than the condition without any strategies; the acquaintance immunization is certified to be more efficient than the random control, basing on the same immunization proportions; the target control further improved the efficiency of immunization strategies; the active control makes up for the deficiency of global information and immunizes the neighbor nodes with a larger degree. In the long term, we will be devoted to exploring more details of human psychological factors in rumor propagation.

Acknowledgements

Project supported by the National Natural Science Foundation of China (Grant No. 62071248) and the Postgradu-

ate Research Innovation Program of Jiangsu Province, China (Grant No. KYCX20_0730).

References

[1] Lin Y, Cai Z, Wang X and F Hao 2019 *IEEE Trans. Veh. Technol.* **68** 9220
[2] Yang L X, Zhang T R, Yang X F, Wu Y B and Yan Y 2018 *J Franklin Inst.* **355** 8079
[3] Vosoughi S, Roy D and Aral S 2018 *Science* **359** 1146
[4] He Z, Cai Z, Yu J, Wang X, Sun Y and Li Y 2017 *IEEE Trans. Veh. Technol.* **66** 2789
[5] Nekovee M, Moreno Y, Bianconi G and Marsili M 2008 *Phys. A* **374** 457
[6] Fei X, Yun L, Zhang Z J, Jiang Z and Zhang Y 2012 *Phys. Lett. A* **376** 2103
[7] Moreno Y, Nekovee M and Pacheco A F 2004 *Phys. Rev. E* **69** 066130
[8] Xia L L, Song Y R, Jiang G P and Bo S 2015 *Phys. A* **437** 295
[9] Wang Y M, Guo T Y, Li W D and Chen B 2020 *Chin. Phys. B* **29** 100204
[10] Zhu H and Ma J 2019 *Phys. A* **513** 257
[11] Wang Z and Chen A 2021 *Complexity* **2021** 6685306
[12] Li J, Hu Y and Jin Z 2019 *Complexity* **2019** 4268393
[13] Huang J and Jin X 2011 *J. Syst. Sci. Complex.* **24** 449
[14] Xia L, Jiang G, Song Y and Bo S 2015 *Entropy* **17** 471
[15] Zhao L, Wang X, Wang J, Qiu X and Xie W 2014 *Discrete Dyn. Nat. Soc.* **2014** 659273
[16] Liu S and Qiu L 2020 *Discrete Dyn. Nat. Soc.* **2020** 5712968
[17] Xu Y, Mei R J, Yang Y J and Kong Z M 2019 *Adv. Math. Phys.* **2019** 7241021
[18] Zhao L, Xie W, Gao H, Qiu X, Wang X and Zhang S 2013 *Phys. A* **392** 6146
[19] Afassinou K 2014 *Phys. A* **414** 43
[20] Huo J and Zhao H 2016 *Phys. A* **448** 41
[21] Sahafizadeh E and Ladani B T 2018 *Phys. A* **506** 412
[22] Huo L, Wang L, Song N, Ma C and He B 2016 *Phys. A* **468** 855
[23] Zhang X W 2014 *J. Comput. Appl.* **34** 411
[24] Chen Z, Tong W, Kausar S and Zheng S 2016 *International Conference on Audio, Language and Image Processing*, July 11–12 2016, Shanghai, China, p. 658
[25] Jin M and Liu F 2019 *IEEE 3rd Information Technology, Networking, Electronic and Automation Control Conference*, March 15–17 2019, Chengdu, China, p. 2256
[26] Zhu X and Liu F 2016 *International Conference on Network and Information Systems for Computers*, April 15–17 2016, Wuhan, China, p. 12
[27] Chua A and Banerjee S 2015 *International Conference on Asian Digital Libraries*, December 9–12 2015, Seoul, Korea, p. 33
[28] F LiuandLi M 2019 *Int. J. Mach. Learn Cyb.* **10** 1449
[29] Wang Y Q, Yang X Y, Han Y L and Wang X A 2013 *Commun. Theor. Phys.* **59** 510
[30] Singh A and Singh Y N 2013 *International Conference on Signal-Image Technology & Internet-Based Systems*, December 2–5 2013, Kyoto, Japan, p. 514
[31] Chen X and Wang N 2020 *Sci. Rep.* **10** 5887
[32] Liu Y, Sanhedrai H, Dong G G, Shekhtman L M, Wang F, Buldyrev S V and Havlin S 2020 *Natl. Sci. Rev.* 8127
[33] Li X, Guo J, Chao G, Zhang L and Zhang Z 2018 *Chaos Soliton Fract.* **106** 214
[34] Xin G E 2011 *Comput. Sci.* **38** 83 (in Chinese)
[35] Fu X C, Michael S, David M W and Zhang H F 2008 *Phys. Rev. E* **77** 036113
[36] F Nian, Hu C, Yao S, Wang L and Wang X 2018 *Chaos Soliton Fract.* **107** 228
[37] Wang J, Zhao L and Huang R 2014 *Phys. A* **398** 43
[38] Cohen R, Havlin S and Ben-Avraham D 2002 *Phys. Rev. Lett.* **91** 247901
[39] Zhu L, Guan G and Li Y 2019 *Appl. Math. Model.* **70** 512
[40] Wang B and Du J 2007 *Communication Studies Course* 2, (Chong Qing: Chong Qing University Press) pp. 92–93 (in Chinese)
[41] Chen Y 2016 *Data Mining Technology and Application* 2 (Beijing: Tsinghua University Press) pp. 94–96 (in Chinese)
[42] Bruno G, Nicola P and Alessandro V 2011 *PLoS One* **6** e22656
[43] Dunbar R 1992 *J. Hum. Evol.* **22** 469
[44] Mirman D 2014 *Chin. Phys. B* **23** 050502
[45] Jiao B and Wu X Q 2017 *Chin. Phys. B* **26** 028901
[46] Wang L Fu, Wang Q L, Kong Z and Jiang Y W 2010 *Chin. Phys. B* **19** 080207
[47] Estrada E and Ross G J 2017 *J. Theor. Biol.* **438** 46
[48] Watts D J and Strogatz S H 1998 *Nature* **393** 440
[49] Barabasi A L, Albert R and Albert R 1999 *Science* **286** 509
[50] Zhang X J and Yang H L 2016 *Chin. Phys. B* **25** 060202
[51] Li M and Wang B H 2014 *Chin. Phys. B* **23** 076402